

# Respiratory motion prediction from CBCT image observations using UKF

Manivannan Sundarapandian  
Siemens Technologies and Services Private Limited  
Bangalore, India  
manivannan.sundarapandiyana@siemens.com

Ramakrishnan Kalpathi  
EE Dept., Indian Institute of Science  
Bangalore, India  
krr@ee.iisc.ernet.in

R Alfredo Siochi  
University of IOWA, Dept. of Radiation Oncology  
Iowa City, IA 52242, USA  
ralfredo-siochi@uiowa.edu

## Abstract

In this paper, we propose a prediction model for breathing pattern based on observations from CBCT raw projection images. From the raw CBCT projections the diaphragm apex position is measured, which in turn is used for the state estimation. We use a novel state space model followed by an Unscented Kalman Filter (UKF). Our method is compared with one of the successful models called Local Circular Motion (LCM). The initial results show that, our model outperforms the LCM model in terms of prediction accuracy.

## 1 Introduction

Adaptive radiotherapy is a challenging topic in External Beam Radiation Therapy (EBRT) wherein the beam is controlled based on the target motion in order to achieve precise delivery. Irrespective of the methods used for target observations there is an inherent latency in the beam control as they involve mechanical movement, processing delays and so on. Hence predicting the target movement at the time of ‘beam on target’ is essential to increase the control precision. We consider the problem of predicting the lung movement based on image based observations. Several methods have been evolved in prediction of respiratory motion [2, 3]. They can be broadly classified into model based and model free methods. *Model-based* approaches use a mathematical model for the breathing motion based on its biomechanical principles whereas the *model-free* approaches rely on heuristic learning. There are various model based approaches in the literature such as linear prediction [4], Finite State Machines [5], sinusoidal [6], state space with Kalman filter and its variants [1].

Ruan et al. [7] used a local regression method to predict the breathing motion, where the breathing state is modeled to be an augmentation of current observation and a set of lagged (past) observations. Hong et al. [8] have developed a model wherein respiratory motion is an one-dimensional projection of a curvilinear motion in a plane augmented with an independent auxiliary axis rather than the delayed axis. They model the local motion along a curvilinear trajectory to be a circular motion (called Local Circular Motion (LCM)). They have used Extended Kalman Filter (EKF) for state estimation, and have tested the prediction performance with observations generated at a rate of 10 Hz.

Herewith we consider an usecase of predicting the breathing pattern based on observing the diaphragm apex from Cone Beam Computed Tomography (CBCT) raw acquisition. Figure 1 shows the diaphragm projection on a raw CBCT image. Apart from applications in adaptive radiotherapy, the predictions are used for motion compensation in CBCT reconstruction to reduce movement artifacts (blur and streaks) [9]. However, the challenge in observing raw CBCT images is that, the frame acquisition rate is less than the sampling rate of other typical external sensors. Typically the sampling rate in case of CBCT is lesser than 10 Hz. For example, Siemens Oncor system acquires 200 frames in about 50 seconds (sample rate of 4 Hz). In such case, the LCM based model does not give the prediction performance as observed in [8]. Herewith, we propose a simple extension of a sine model to represent the breathing motion. With this model we use an Unscented Kalman Filter and show that our prediction algorithm outperforms the LCM model and EKF combination.



Figure 1. CBCT raw image

## 2 Materials and methods

### 2.1 Stochastic filters

The problem of stochastic filtering is to estimate the optimal state  $\mathbf{x}_k$  of a dynamic system at time  $k$  given the observations  $\mathbf{z}_k$  up to time  $k$ , the state and measurement models and the initial density  $p(\mathbf{x}_0)$  of the state. A dynamic system in state space form with additive noise is represented by the two equations:  $\mathbf{x}_k = \mathbf{f}_{k-1}(\mathbf{x}_{k-1}, k-1) + \mathbf{q}_{k-1}$ ;  $\mathbf{z}_k = \mathbf{h}_k(\mathbf{x}_k, k) + \mathbf{r}_k$ , where  $\mathbf{f}_k$ ,  $\mathbf{h}_k$  are the system and measurement functions respectively.  $\mathbf{q}_k$  and  $\mathbf{r}_k$  are the process noise and observation noise. Kalman filter is an example of an optimal state estimator in the mean squared sense when the system and measurement models ( $\mathbf{f}$  and  $\mathbf{h}$ ) are linear and when  $\mathbf{q}$  and  $\mathbf{r}$  are additive Gaussian. The recursive filter equations are given by

$$\hat{\mathbf{x}}_k^- = E[\mathbf{f}_{k-1}(\hat{\mathbf{x}}_{k-1}, k-1) + \mathbf{q}_{k-1}] \quad (1)$$

$$\widehat{\mathbf{z}}_k^- = E \left[ \mathbf{h}_{k-1}(\widehat{\mathbf{x}}_k^-, k) + \mathbf{r}_k \right] \quad (2)$$

$$\widehat{\mathbf{x}}_k = \widehat{\mathbf{x}}_k^- + K_k \left[ \mathbf{z}_k - \widehat{\mathbf{z}}_k^- \right] \quad (3)$$

where  $\widehat{\mathbf{x}}_k^-$  and  $\widehat{\mathbf{z}}_k^-$  are the optimal predicted state and the optimal predicted observation respectively at time  $k$ .  $K_k$  is known as Kalman gain given by  $K_k = P_{x_k v_k} P_{v_k v_k}^{-1}$  where  $\mathbf{v}_k = \mathbf{z}_k - \widehat{\mathbf{z}}_k^-$ .  $P$  represents the covariance matrix of the random vectors (given in the subscript).

Extended Kalman Filters (EKF), Particle Filters (PF) are used in applications wherein  $\mathbf{f}$  and  $\mathbf{h}$  are non-linear, or  $\mathbf{q}$  and  $\mathbf{r}$  are non-Gaussian. EKF has the following approximations: state distribution assumed to be Gaussian; expectation operators are dropped in (1),(2); Taylor series expansions are used for  $\mathbf{f}$  and  $\mathbf{h}$ . Although EKFs are successful in many applications, these approximations increase the computational effort [10], [1], and give suboptimal performance in some cases [11]. PF implements the recursive steps using (sequential) Monte Carlo methods. The posterior pdf of the state is represented by a set of samples called particles. However, computing the particle weights (based on the likelihood function) is a challenge as there are many spurious artifacts in the CBCT gradient image, even after the preprocessing step (refer Fig. 3b).

### 2.1.1 Unscented Kalman Filter

In case of Unscented Kalman Filter (UKF), the state distribution is assumed to be Gaussian; it is represented using a minimal set of sample points, called sigma points. The sigma points capture the true mean and the covariance of the Gaussian variables. However, they are propagated through the true non-linear system  $\mathbf{f}$  and  $\mathbf{h}$  (unlike the EKF, wherein they are approximated to be linear).

The Unscented Transform (UT) is a method to compute the statistics (mean and covariance) of a random vector  $\mathbf{x}$  transformed through a non-linear function  $\mathbf{y} = g(\mathbf{x})$ . Based on the dimension  $L$  of  $\mathbf{x}$ ,  $2L + 1$  sigma points  $\mathcal{X}_i$  are selected that are representative of the distribution of  $\mathbf{x}$ .  $\mathcal{X}_i$  are selected in and around the mean  $\bar{\mathbf{x}}$ , based on the covariance  $P_{\mathbf{x}}$  of  $\mathbf{x}$ . The sigma points are associated with weighting factors  $W_{mi}$  and  $W_{ci}$  for mean and covariance respectively. Refer [11] for detailed expressions of  $\mathcal{X}_i$  and weights  $W_{mi}$  and  $W_{ci}$ . The mean  $\bar{\mathbf{y}}$  and covariance  $P_{\mathbf{y}}$  are approximately given by

$$\bar{\mathbf{y}} \approx \sum_{i=0}^{2L} W_{mi} g(\mathcal{X}_i) \quad (4)$$

$$P_{\mathbf{y}} \approx \sum_{i=0}^{2L} W_{ci} [g(\mathcal{X}_i) - \bar{\mathbf{y}}] [g(\mathcal{X}_i) - \bar{\mathbf{y}}]^T \quad (5)$$

The filter estimates  $\mathbf{x}_k$  recursively using (3) and uses UT approach to propagate  $\mathbf{x}_k$  through nonlinear functions  $\mathbf{f}$  and  $\mathbf{h}$  [11].

## 2.2 Non-linear models

We now review two models that are used to estimate quasi-periodic signals.

### 2.2.1 LCM model

The LCM model is based on the assumption that, a planar curve can be approximated by a circular arc locally. Here the breathing pattern is modeled as the 1D-projection of the path of a point object that moves in circles, in an augmented coordinate system. The state vector for LCM model has four components  $\{x, \dot{x}, \dot{y}, \omega\}$ .  $x$  is the projection of the path along  $x$ -axis. The speed ( $\dot{x}$  and  $\dot{y}$ ) and angular velocity ( $\omega$ ) of the object evolve over time, based on observation. The state equations are,  $\ddot{x} = -\omega \dot{y}$ ,  $\ddot{y} = \omega \dot{x}$ ,  $\dot{\omega} = 0$ . In discretized form, the state vector for the LCM model is  $\mathbf{x}_k = [x_k, \dot{x}_k, \dot{y}_k, \omega_k]^T$ . We refer to [8] for the details of deriving discrete state equations, noise models and present only the final equations herewith. The discretized state equation in matrix form is

$$\mathbf{x}_k = \begin{pmatrix} 1 & \frac{\sin(\omega_k T)}{\omega_k} & -\frac{1 - \cos(\omega_k T)}{\omega_k} & 0 \\ 0 & \cos(\omega_k T) & -\sin(\omega_k T) & 0 \\ 0 & \sin(\omega_k T) & \cos(\omega_k T) & 0 \\ 0 & 0 & 0 & 1 \end{pmatrix} \mathbf{x}_{k-1} + \mathbf{q}_{k-1}$$

where  $T$  is the sampling step size (based on sampling rate). The discretized process noise  $\mathbf{q}_{k-1}$  is assumed to be  $N(\mathbf{0}, \mathbf{Q})$ . It adds randomness to  $\dot{x}_k, \dot{y}_k, \omega_k$ . The respective spectral densities are  $q_1, q_2, q_3$ . The observation model is given by  $\mathbf{h}(\mathbf{x}_k, k) = x_k + r_k$ , where  $r_k \sim N(0, \sigma_r)$ . That is, the model ‘observes’ the first component of the state vector, which is a sine function. The configurable parameters of this model are  $\{q_1, q_2, q_3, \sigma_r\}$ .

### 2.2.2 Sine model

In *sine model*, the state vector has three components  $\{\theta, \omega, a\}$  corresponding to a sine wave. The amplitude  $a$  and the angular velocity  $\omega$  vary randomly to model the quasi-periodicity;  $\frac{d\theta}{dt} = \omega$ , where  $\theta$  is the phase. We refer to [10] for the details of deriving state equations, noise models and present only the final equations herewith. In discretized form, the state vector for the *sine model* is  $\mathbf{x}_k = [\theta_k, \omega_k, a_k]^T$ . The discretized state equation in matrix form is given by,

$$\mathbf{x}_k = \begin{pmatrix} 1 & T & 0 \\ 0 & 1 & 0 \\ 0 & 0 & 1 \end{pmatrix} \mathbf{x}_{k-1} + \mathbf{q}_{k-1}$$

The discretized process noise  $\mathbf{q}_{k-1}$  is assumed to be  $N(\mathbf{0}, \mathbf{Q})$ . It adds randomness to  $\omega_k$  and  $a_k$ . The respective spectral densities are  $q_1, q_2$ . The observation equation is:  $\mathbf{h}(\mathbf{x}_k, k) = a_k \sin(\theta_k) + r_k$ , where  $r_k \sim N(0, \sigma_r)$ . That is, the model ‘observes’ the sine wave from the state components  $a_k$  and  $\theta_k$ . The configurable parameters of this model are  $\{q_1, q_2, \sigma_r\}$ .

## 2.3 Our model

Our model called as ‘offset-sine model’ is a variant of the *sine model* given above. The components of the state vector and the state equation are identical to that of the *sine model*, however, with different interpretations. The observation equation includes two biases with respect to the state components  $a_k$  and  $\theta_k$ . They

are estimated separately prior to the state estimator (refer Fig. 2).

This model is driven by the fact that, the breathing signal has a base pattern from which its amplitude and frequency drift randomly. Estimating these parameters in the first stage limits the process noise to an extent corresponding to the parameter deviations.

The observation equation is:

$$\mathbf{h}(\mathbf{x}_k, k) = a_0 + a_k \sin(\omega_0 k + \theta_k) + r_k.$$

The component  $a_k$  models the amplitude of the non-zero frequency component from the base level;  $\theta_k$  and  $\omega_k$  model the differential phase and the frequency in the pattern from the base frequency. The amplitude bias  $a_0$  can be estimated from the initial measurement. The base frequency  $\omega_0$  can be estimated as follows:

- (i) From the observed set of samples find the time corresponding to the positive peak (based on the instance of sign change in the time derivative).
- (ii) From the consecutive times of positive peaks determine the wave duration.
- (iii) Based on multiple wave durations found earlier compute  $\omega_0 = 2\pi/T_0$ , where  $T_0$  is the average duration.

We note that the deviations in the predicted state vector  $\hat{\mathbf{x}}_k^-$  (from  $\hat{\mathbf{x}}_{k-1}^-$ ) for a given change in  $\hat{\mathbf{z}}_k^-$  from  $\hat{\mathbf{z}}_{k-1}^-$  is much lesser in our model compared to that of LCM.

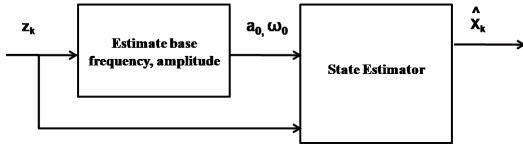


Figure 2. Schematic block of estimator

### 2.3.1 UKF based prediction

We use UKF for motion prediction and estimation of the state. The state vector  $\mathbf{x}_k$  represents the vertical position of the diaphragm apex. The observation  $\mathbf{h}$  gives the vertical position of the diaphragm apex. The state vector has 3 dimensions, hence the UKF uses 7 sigma points. The UKF steps are similar to that of Kalman Filter. The mean and covariance computations in the prediction and the estimation steps are achieved through the Unscented Transform given in Sec.2.1.1. With  $\mathbf{h}$  being non-linear, UKF is naturally a better alternative to EKF, as it propagates the mean and covariance with higher accuracy than EKF.

### 2.3.2 Measurement of Diaphragm apex position

We use a Hough Transform based approach to measure the position of the diaphragm apex on the CBCT images. The diaphragm shape was modeled as a pair of piecewise smooth asymmetric parabolic sections with a common apex point  $(p_x, p_y)$ . Hence the Hough space is a 4D-space with parameters  $(p_x, p_y, f_l, f_r)$ , where  $f_l, f_r$

are the focal length parameters of the left and right parabolic sections respectively. Figure 3a shows curves (asymmetric parabolas) corresponding to few points in the Hough space. The raw CBCT image was pre-processed with an anisotropic filter followed by Sobel operator to obtain the gradient image. The Hough space is computed using the gradient image, and the point having maximum vote is identified as the diaphragm boundary. Figure 3b shows the gradient image and the detected shape (as a black overlay) through Hough transform. The vertical coordinate  $p_y$  of the detected apex position at  $k$  was used as  $\mathbf{z}_k$ .

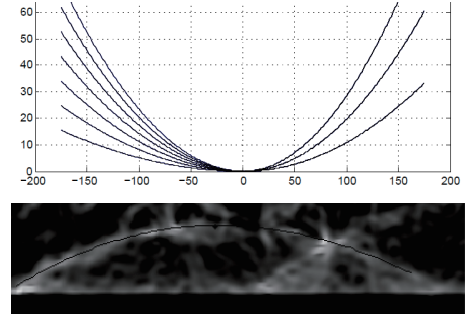


Figure 3. (a) asymmetric parabolic shapes (b) diaphragm detection

## 3 Experiments and results

We have developed a prototype of our algorithm on a dual Pentium machine, with 2.4 GHz, 2GB RAM, as hardware. We have implemented the offset-sine model with UKF using MATLAB. We used the code base, libraries from [10] for implementing the filters. The reference model (LCM with 1st order EKF) was implemented and configured as in [8].

We used 15 CBCT images acquired from multiple patients, using Siemens Oncor LINAC system. Each CBCT image consists of 200 frames (orbital projections) acquired over the gantry movement from 270 degree to 110 degree clockwise. The specifications of the imager are: the acquisition rate is 4 Hz (200 frames/50 sec), the Source to Imager Distance (SID) is 145 cm; pixel resolution is  $0.27 \times 0.27$  sq.mm.

Hong et al [8] have used breathing patterns generated from real position management system (RPM) as measured data  $\mathbf{z}_k$ . Their prediction accuracies were reported based on comparisons against  $\mathbf{z}_k$ . We measured  $\mathbf{z}_k$  using Hough transform approach as described in Sec 2.3.2. The ground truth  $\zeta_k$  of the diaphragm apex position was marked on the raw images by an experienced radiotherapy doctor. The prediction accuracy is computed with respect to  $\zeta_k$ .

For offset-sine model, the configurable parameters were  $q_1 = 0.2$ ,  $q_2 = 5$ ,  $\sigma_r = 1.5$ .  $a_0$  was initialized with the first observation of  $\mathbf{z}$ . We took an average angular frequency for a given trace (breathing pattern) and initialized  $\omega_0$  for that dataset.

Figure 4 illustrates the predictions using our approach and compares the same with that of the reference model. It can be seen that both the models show similar performance while the waveforms have similar amplitude (peak-to-peak levels). However, when there

Table 1. Comparison of the nRMSEs between the models

| Dataset | LCM+EKF | our model |
|---------|---------|-----------|
| 1       | 0.4082  | 0.3412    |
| 2       | 0.2130  | 0.1926    |
| 3       | 0.6765  | 0.3636    |
| 4       | 1.2544  | 0.3097    |
| 5       | 0.3100  | 0.2560    |
| 6       | 0.3214  | 0.2830    |
| 7       | 1.2536  | 0.3202    |
| 8       | 0.5210  | 0.3283    |
| 9       | 1.1765  | 0.3312    |
| 10      | 0.5948  | 0.3254    |
| 11      | 0.3945  | 0.3829    |
| 12      | 0.2184  | 0.2085    |
| 13      | 0.2480  | 0.2211    |
| 14      | 0.2979  | 0.2482    |
| 15      | 0.7961  | 0.3009    |

is a change in amplitude, our model has less overshoot compared to the reference model.

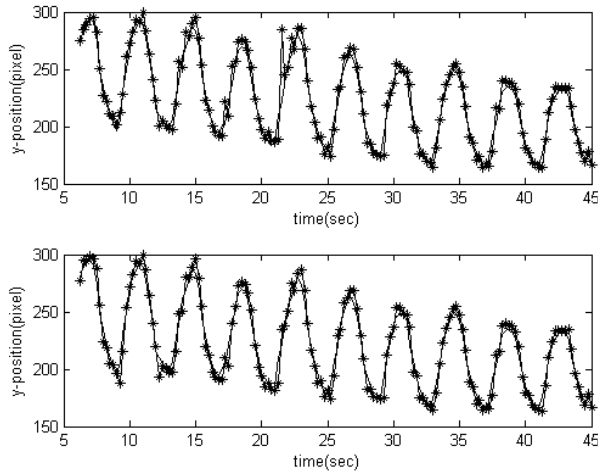


Figure 4. Comparison of prediction performance between LCM+EKF (top) and Offset-sine+UKF model (bottom)

The quality of prediction is measured through normalized root mean squared error (nRMSE).

$$nRMSE = \sqrt{\frac{1}{|\mathcal{N}|} \sum_{k \in \mathcal{N}} (\hat{\mathbf{z}}_k - \zeta_k)^2 / \sigma_{\mathbf{z}}}$$

where the numerator is the RMS value of the prediction error over a duration  $\mathcal{N}$ . The RMS value of the observation is denoted by  $\sigma_{\mathbf{z}}$ .  $nRMSE$  indicates the prediction accuracy at  $k$  based on the observation at  $k-1$ , for all the observations. Table 1 shows the values of nRMSE computed for our solution and the reference model for all the 15 dataset. It is observed that in all the dataset, nRMSE was lesser in case of offset-sine model+UKF than that of the reference model. For three traces, the reference model has lost the track, which could be possibly due to low sampling frequency (4Hz). Another observation is that, when there are

changes in the pattern (either in the peak-to-peak levels or in the waveform duration) our model performs better than the reference model. We need to perform extensive validation to characterize this in detail.

## 4 Summary

This paper has proposed a new model for predicting the breathing pattern from the observations of CBCT images. Our model uses UKF, which is a better alternative to EKF for state estimation of non-linear dynamic systems. Initial studies with clinical dataset indicates that, our approach outperforms the LCM + EKF model, and can operate at a data rate of 4Hz applicable for CBCT acquisition. We need to perform extensive validation to arrive at the optimal configuration parameters of our model. We will take up this as our future work.

## References

- [1] B.-H. Jung, B.-H. Kim, and S.-M. Hong, "Respiratory motion prediction with extended kalman filters based on local circular motion model." *International Journal of Bio-Science and Bio-Technology*, vol. 5, pp. 51–58, 2013.
- [2] S. J. Lee and Y. Motai, "Review: Prediction of respiratory motion," in *Prediction and Classification of Respiratory Motion*. Springer, 2014, pp. 7–37.
- [3] J. R. McClelland, D. J. Hawkes, T. Schaeffter, and A. P. King, "Respiratory motion models: A review," *Medical image analysis*, vol. 17, no. 1, pp. 19–42, 2013.
- [4] G. C. Sharp, S. B. Jiang, S. Shimizu, and H. Shirato, "Prediction of respiratory tumour motion for real-time image-guided radiotherapy," *Physics in medicine and biology*, vol. 49, no. 3, p. 425, 2004.
- [5] H. Wu, G. C. Sharp, B. Salzberg, D. Kaeli, H. Shirato, and S. B. Jiang, "A finite state model for respiratory motion analysis in image guided radiation therapy," *Physics in Medicine and Biology*, vol. 49, no. 23, p. 5357, 2004.
- [6] S. Vedam, P. Keall, A. Docef, D. Todor, V. Kini, and R. Mohan, "Predicting respiratory motion for four-dimensional radiotherapy," *Medical physics*, vol. 31, no. 8, pp. 2274–2283, 2004.
- [7] D. Ruan, J. A. Fessler, and J. Balter, "Real-time prediction of respiratory motion based on local regression methods," *Physics in medicine and biology*, vol. 52, no. 23, p. 7137, 2007.
- [8] S. Hong, B. Jung, and D. Ruan, "Real-time prediction of respiratory motion based on a local dynamic model in an augmented space," *Physics in medicine and biology*, vol. 56, no. 6, p. 1775, 2011.
- [9] S. Rit, J. W. Wolthaus, M. van Herk, and J.-J. Sonke, "On-the-fly motion-compensated cone-beam ct using an a priori model of the respiratory motion," *Medical physics*, vol. 36, no. 6, pp. 2283–2296, 2009.
- [10] J. Hartikainen, A. Solin, and S. Särkkä, "Optimal filtering with kalman filters and smoothers," *Department of Biomedical Engineering and Computational Sciences, Aalto University School of Science, 16th August*, 2011.
- [11] E. A. Wan and R. Van Der Merwe, "The unscented kalman filter for nonlinear estimation," in *Adaptive Systems for Signal Processing, Communications, and Control Symposium 2000. AS-SPCC. The IEEE 2000*. IEEE, 2000, pp. 153–158.